Coral Reefs
https://doi.org/10.1007/s00338-021-02205-8

REPORT

Strong genetic structure and limited connectivity among populations of Clark's Anemonefish (*Amphiprion clarkii*) in the centre of marine biodiversity

Hugo Ducret[1] · Janne Timm[2] · Melina Rodríguez-Moreno[3] · Filip Huyghe[1] · Marc Kochzius[1]

Received: 15 March 2021 / Accepted: 24 November 2021

Abstract Populations of anemonefish species often show signs of local isolation due to limited dispersal potential and oceanographic conditions. Additionally, anthropogenic pressure, such as overharvesting and coral reef exploitation causes reduced population size, eventually leading to local extinction. The understanding of the genetic population structure, as well as the influence of both historical and current connectivity, is required to design effective marine protected area (MPA) networks. In this study, the genetic structure of Clark's Anemonefish *(Amphiprion clarkii*) based on 209 individuals from 16 samples sites in the Indo-Malay Archipelago (IMA) is assessed through mitochondrial control region (mtCR) sequences and eight nuclear microsatellite loci. Results provided evidence of a significant genetic structure (mtCR: $\Phi_{st} = 0.42$, $\Phi_{ct} = 0.64$; microsatellites: $F_{st} = 0.01$, $F_{ct} = 0.05$). Genetic breaks were identified among Western (Padang Karimunjawa), Central (Sulawesi, Borneo, Bali, Komodo, Timor) and Eastern (Biak) IMA populations, with almost no gene flow. This matches with patterns obtained for congeneric and other coral reef taxa. Due to the restricted connectivity among these three regions, it is suggested to consider them as separate management areas in the design of MPA networks.

Keywords Clownfish · Coral Triangle · Indonesia · Phylogeography · Marine conservation

Topic Editor Peter Francis Cowman

✉ Marc Kochzius
Marc.Kochzius@vub.be

[1] Marine Biology, Ecology and Biodiversity, Vrije Universiteit Brussel (VUB), Pleinlaan 2, 1050 Brussels, Belgium

[2] Molecular Genetics and Biotechnology, Universität Bremen, Bibliothekstraße 1, 28359 Bremen, Germany

[3] Department of Biology, Universidad del Valle, Ciudad Universitaria Meléndez Calle 13 # 100-00, 760000 Cali, Colombia

Introduction

The anemonefish *Amphiprion clarkii* is a small reef fish species of the family Pomacentridae, commonly encountered in tropical shallow waters of the Indo-Pacific. Though juvenile individuals settle in coastal waters onto host sea anemones, larvae are planktonic and their movement can be strongly influenced by sea surface currents (SSC), allowing them to disperse (Simpson et al. 2014). The pelagic larval duration (PLD) of *A. clarkii* is rather short (16–24 d, Ye et al. 2011), suggesting restricted dispersal potential. This notion is supported by several studies reporting very high levels of self-recruitment in anemonefish that varies among species, location and season (*Amphiprion polymnus* 15.9–31.5%, Jones et al. 2005; *A. percula* 40–60%, Almany et al. 2007, Planes et al. 2009; *A. chrysopterus* 27%, Beldade et al. 2012; *A. perideraion* 46.9%, *A. ocellaris* 48%, Madduppa et al. 2014a). A study in the Philippines (central Visayas) using genetic and population density data estimated a dispersal distance of about 11 km for *A. clarkii* (Pinsky et al. 2010). These ecological features are likely leading to locally isolated populations that exchange very few migrants, with populations prone to reduced population size. This is shown for populations of *A. ocellaris*, which are under high fishing pressure for marine ornamental trade (Madduppa et al. 2014a, b, 2018). Anemonefishes are popular in the aquarium trade, and if too many individuals are harvested at a

Published online: 17 January 2022

certain location, and no migration from other populations occurs, the population eventually disappears. These threats increase the need of understanding the patterns shaping the dynamic of these species and designing proper Marine Protected Area (MPA) networks.

The development of molecular ecology tools allows to understand the patterns shaping the genetic diversity of several *Amphiprion* species, particularly within the Indo-Malay Archipelago (IMA). Indeed, population genetic studies have already identified several genetic breaks shared by two anemonefish species within the IMA (*A. ocellaris*: Timm and Kochzius 2008; Timm et al. 2012; *A. perideraion*: Dohna et al. 2015), but also other coral reef taxa (giant clams: Kochzius and Nuryanto 2009; Nuryanto and Kochzius 2009; Hui et al. 2016, 2017; corals: Knittweis et al. 2009; van der Ven et al. 2021; sea star: Crandall et al. 2008; Kochzius et al. 2009; reef fish: Ackiss et al. 2013; Raynal et al. 2014). These barriers distinguish several clusters of populations from each other, based on their genetic structure. Most of the studies revealed the existence of two genetic breaks across the IMA, separating three groups of populations from each other. The first one comprises populations from the Western IMA (Eastern Indian Ocean, Java Sea), while the second one includes populations from the Central IMA (Sulawesi Sea, Makassar Strait, Flores Sea, Banda Sea, Maluku Sea and Sawu Sea) and the third one concerns populations from the Eastern IMA (Seram Sea and Western Pacific). However, the genetic population structure of *A. clarkii* remains unknown in this region. The ecological properties of each species often lead to relatively different differentiation patterns (Timm and Kochzius 2008; Dawson 2014; Dawson et al. 2014; Dohna et al. 2015). More information about the genetic structure of *A. clarkii* is needed in order to apply effective conservation plans adapted to this species.

The aim of this study was to assess the genetic structure of *A. clarkii* across the IMA using genetic markers. As ecological differences between sister species might lead to distinct differentiation patterns, a different pattern of genetic structure was expected for Clark's anemonefish compared to its congeners as a result of its longer PLD (Ye et al. 2011; Dawson 2014). However, as for its congeners, it was assumed to find highly structured populations and a high genetic diversity in accordance with the life cycle of this demersal species with substrate-attached eggs and limited pelagic larval dispersal. The conservation of endangered species with such life histories requires in-depth studies providing explicit information regarding genetic structure. Therefore, this study will aim at examining the genetic differentiation occurring between populations of Clark's anemonefish and identify potential genetic breaks among them. This will reveal the location of diversity hotspots for this species and provide the required information for its conservation and the design of management plans.

Materials and methods

DNA extraction and amplification

A total of 209 fin clip samples of Clark's anemonefish were collected at 16 sample sites across the IMA using SCUBA diving and stored in 96% ethanol at 4 °C. Genomic DNA was extracted with a commercial kit (peqGOLD Tissue DNA Mini Kit, Peqlab, Erlangen) following the manufacturer's instructions. A 420-bp fragment of the D-loop segment of the mitochondrial control region (mtCR) was amplified with the primers CR-A (TTC CAC CTC TAA CTC CCA AAG CTA G) and CR-E (CCT GAA GTA GGA ACC AGA TG) (Lee et al. 1995) for all the individuals in the dataset, following a standard protocol detailed in Timm and Kochzius (2008): The 25-µL reaction volume of the PCRs contained 2.5 µL 10 × PCR buffer, 0.075 µmol Mg^{2+}, 0.25 µmol dNTP mix, 10 pmol of each primer, 0.5 U Taq Polymerase and 10–30 ng genomic DNA of each sample. The temperature profile of the PCR was 95 °C for 2 min, followed by 35 cycles of 95 °C for 30 s, 50 °C for 30 s and 72 °C for 60 s, and the terminal elongation at 72 °C for 2 min. Finally, PCR products were purified with the QIA quick PCR purification kit (Qiagen), and both strands were sequenced on an ABI Automated Sequencers (Applied Biosystems) using the PCR primers.

Eight polymorphic microsatellite loci were amplified for all the 209 individuals at each location. Primers were either FAM- or HEX- labelled and the PCR protocol used by Timm et al. (2012) was also used in the current study (Table 1): the reaction volume of 10 µl contained 1 µl 10 × PCR buffer, 0.0125 µmol Mg^{2+}, 0.002 µmol dNTP mix, 5 pmol of each primer, 0.1 U Taq polymerase and 10–20 ng genomic DNA of each sample for each locus. The thermal profile was as follows: 94 °C for 2 min, followed by 35 cycles of 94 °C for 45 s, the primer specific annealing temperature (Table 1) for 45 s, and 72 °C for 60 s, with a 2-min-long terminal elongation at 72 °C. Fragment lengths were subsequently measured with an ABI Automated Sequencers (Applied Biosystems) and analysed with the software Genemapper (Applied Biosystems).

Control region

Neutrality of the mtCR marker was evaluated to ensure suitability for population genetic analyses. Tajima's D (Tajima 1989) and Fu's F_s (Fu 1997) were used to detect recent population expansion or bottlenecks.

Table 1 Polymorphic microsatellites loci used for the analysis of the anemonefish *Amphiprion clarkii* from the Indo-Malay Archipelago

Locus	Motif	Product size (bp)	No. alleles	Primers	Ann. temp. (°C)	H_o	H_e	Source (*Amphiprion* sp.)
Ac1578	$(AC)_9$	242–266	13	F: 5′-CAGCTCTGTGTGTGTTTAATGC-3′ R: 5′-CACCCAGCCACCATATTAAC-3′	55.7	0.997	0.789	*A. clarkii* (Liu et al. 2007)
Ac626	$(TC)_6(AC)_{20}$	222–270	25	F: 5′-CACACATGCACACACCTTGA-3′ R: 5′-TAATTGAGGCAGGTGGCTTC-3′	60	0.985	0.780	*A. clarkii* (Liu et al. 2007)
Ac137	$(AC)_{19}$	274–334	31	F: 5′-GGTTGTTTAGGCCATGTGGT-3′ R: 5′-TTGAGACACACTGGCTCCT-3′	55.7	0.972	0.852	*A. clarkii* (Liu et al. 2007)
CF27	$(TCTA)_{16}$	185–229	12	F: 5′-AAGCTCCGGTAACTCAAAACTAAT-3′ R: 5′-GTCATCTGATCCATGTTGATGTG-3′	60	1.000	0.851	*A. percula* (Buston et al. 2007)
65	$(GT)_{12}$	243–263	10	F: 5′-TGAACACATAAACGCTCACTCAC-3′ R: 5′-AAGACAATGCCTCCACATATCTA-3′	58.7	0.924	0.856	*A. ocellaris* (Quenouille et al. 2004)
45	$(GT)_{35}$	212–246	19	F: 5′-TTGGAGCAGCGTACTTAGCT-3′ R: 5′-AGATGTGTTTACGCACGCTT-3′	58.7	1.000	0.780	*A. ocellaris* (Quenouille et al. 2004)
AC27	$(GT)_7GA(GT)_{11}$	210–242	15	F: 5′-TTTGCTCTTGTGGGGAGTTC-3′ R: 5′-TGTTCTCTAGTGGGGGTGGA-3′	62	1.000	0.708	*A. clarkii* (Liu et al. 2007)
AC1359	$(AC)_9$	229–257	17	F: 5′-TGAAATACGATGCGGAAACA-3′ R: 5′-GAAGGCGAATACGTGGGATA-3′	53	0.932	0.765	*A. clarkii* (Liu et al. 2007)

Observed (Ho) and expected (He) heterozygosities are indicated for each locus

Ann. Temp, annealing temperature for PCR

Unless otherwise stated, all following analyses were carried out with Arlequin (v. 3.5). For mtCR, nucleotide and haplotype diversities were assessed for each sample site (Nei 1987). The overall genetic population structure (Φ_{st}), as well as pairwise population differentiation (pairwise Φ_{st}), was established through an Analysis of Molecular Variance (AMOVA). The matching *p*-values obtained with computations were adjusted regarding the false discovery rate (FDR) following Benjamini and Hochberg's procedure (1995) (multtest, R package 2.9.0). Groups for hierarchical AMOVA testing were chosen to depict regional clustering based on population differentiation, which significance was obtained according to a *p*-value. Different scenarios were tested according to pairwise Φ_{st}-values obtained with the AMOVA.

A haplotype network was constructed from 209 mtCR DNA sequences with the software TCS (v.1.2.1; Clement et al. 2000). All haplotypes were included in the haplotype network, from which haplogroups were identified. They were defined as containing less mutational steps within than among them, and single outlier haplotypes were not defined as haplogroups as their position in the haplotype network is questionable (Dohna et al. 2015). The graphical output shown in Fig. 1a was drawn by hand on the basis of what was obtained with TCS. Pie charts show the relative frequency of each haplogroup in each population in Fig. 1b.

The program IM (Hey and Nielsen 2007) was used to provide estimates of bidirectional gene flow among pairs of populations across genetic barriers. It is based on a Bayesian approach and uses Monte Carlo Markov chain (MCMC) algorithms to plot posterior densities of demographic parameters for a pair of populations. The burn-in period was set to 100,000, steps and the total length was set to 10,000,000 steps. Each analysis was run twice with the same settings and different random seed numbers to crosscheck the results. The peaks of the observed distributions were taken as the approximated values of the parameters. To improve mixing and therefore chain convergence, the Metropolis coupling method was used and the program was run with $n = 13$ chains with distinct heated states. Different heating modes are implemented by the program, in which chain number i will be assigned a heating term $0 < \beta_i < 1$, 1 being the heating term of the cold chain and 0 the maximum heating term. Each heating mode was tested, and the one providing the best mixing was kept. Therefore, a geometric heating mode was chosen to run the analysis, with a degree of nonlinearity:

$$h_1 = \left(\frac{(1-\beta_1)*(n-1)}{(1-h_2)}\right)^{\frac{1}{n-2}} = 0.727$$

where $h_2 = \beta_{n-1} = 0.6$ (Hey and Nielsen 2007) and $\beta_1 = 0.995$. Effective sample size (ESS) values given by the program for parameter estimate were monitored over

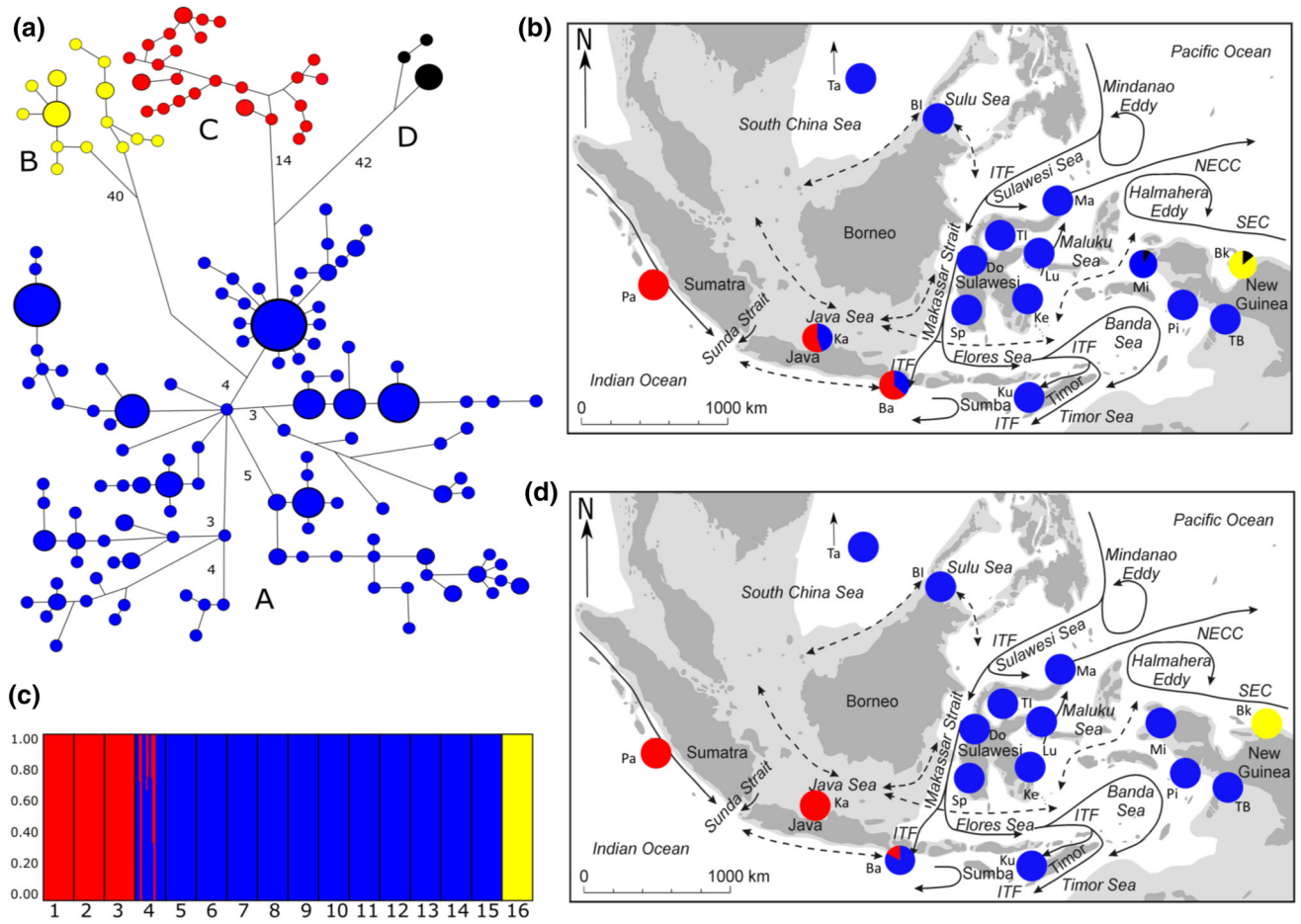

Fig. 1 **a** Haplotype network of the anemonefish *Amphiprion clarkii* based on 209 mtCR DNA sequences. The size of the coloured circles is relative to the number of individuals represented by that haplotype. The smallest coloured circles represent one individual, while the biggest represent eight individuals. Connecting lines without numbers mean one mutational step between haplotypes, and additional mutations are indicated by numbers. **b** Map showing the distribution of the haplogroups identified throughout the populations of the Indo-Malay Archipelago (IMA). **c** Bar plot calculated with the software STRUCTURE for all of the 16 populations (1 = Padang, 2 = Karimunjawa, 3 = Bali, 4 = Spermonde, 5 = Donggala, 6 = Banggi Islands, 7 = Taiwan, 8 = Togian Islands, 9 = Manado, 10 = Luwuk, 11 = Kupang, 12 = Kendari, 13 = Misol, 14 = Pisang, 15 = Triton Bay, 16 = Biak), with $K = 3$. **d** Map showing the distribution of the microsatellite genotype clusters identified with STRUCTURE for the populations of the IMA. For both maps, arrows indicate major surface currents, dashed arrows depict seasonally reversing currents, dark grey areas are present-day land formations, and light grey shading indicates marine habitat exposed during the Pleistocene glacial maxima, which led to a 120 m drop in sea level (Voris 2000). ITF: Indonesian Throughflow; NECC: Northern Equatorial Counter Current; SEC: Southern Equatorial Current

the course of a run to assess chain convergence. The rule of thumb is that the minimal ESS values should be above 50 to consider chain convergence as successful.

Microsatellites

Samples showing multi-locus matches were excluded from the dataset prior to further analysis. Expected and observed heterozygosities in each population and overall were assessed, as well as tests of significant deviations from Hardy–Weinberg equilibrium in the distribution of alleles. A likelihood ratio test was performed to detect linkage disequilibrium between pairs of loci (Slatkin and Excoffier 1996). Obtained p-values were corrected according to Benjamini and Hochberg (1995), accounting for FDR. All loci were assessed with Microchecker (v. 2.2.3) to assess the number of null alleles and potential allele dropout. Mean gene diversity was assessed for each population, and genetic differentiation was derived through pairwise D_{est}-values for each population (Wright 1965). Their significance was given by p-values estimated from bootstrap resampling with 1000 permutations.

Hierarchical AMOVA testing was also applied to microsatellites, in order to depict regional clustering based on population differentiation. Different scenarios were tested according to pairwise F_{st}-values obtained with the

AMOVA. The genetic structure of Clark's anemonefish was then further investigated through the program STRUCTURE (v. 2.3.3). This method uses a maximum likelihood approach to estimate the probability of accordingly dividing all the genotypes of individuals from n populations among k clusters, $k = \{1, \ldots, n\}$. The burn-in period was set to 100,000 iterations, and total length was set to 500,000 steps with 10 repetitions for each k-value. The distribution of the genetic clusters across populations is represented in Fig. 1d.

Results

The mitochondrial control region sequences are available at GenBank (Accession numbers OL943590-OL943794).

Neutrality tests of the genetic markers

A non-significant test of Tajima's D failed to reject the neutrality of the mitochondrial control-region marker ($p > 0.1$), thus confirming its suitability for the current analysis (Table S1). Besides that, the non-significant Fu's F_s outcome provided no evidence of departure from population equilibrium, such as recent population expansion (considered significant at the 2% level). The mismatch distribution plot (Supplementary Fig. S1) confirms this result through a decreasing curve of expected mismatch distribution. The presence of three peaks in the observed mismatch distributions may represent substructures within the dataset (Ray et al. 2003). However, both the sum of square deviations (SSD) and Harpending's raggedness index showed no deviation from a model of sudden demographic expansion.

Regarding microsatellites, observed heterozygosities were consistently high (Table 1, 0.9–1), each time higher than the respective expected heterozygosities. The highest number of alleles obtained was 31 for locus AC137. Little evidence of null alleles was found, the highest obtained occurrence was 24% for CF27. No locus displayed consistent deviations from Hardy–Weinberg equilibrium (HWE) (ChiSq > 0.05, results not shown), confirming their suitability for population genetic studies. Additionally, no population showed a consistent deviation from HWE across loci, so violation of model assumptions for 'ideal' populations is unlikely. Tests of linkage disequilibrium across pairs of loci indicate three pairs of linked loci (AC27-AC1578; AC27-AC626; 65-AC1359) across four populations (Biak, Togian Islands, Manado, Donggala). This linkage is expected to carry across populations if these markers are truly linked, which is not the case here. Therefore, all loci were expected to assort independently and were used in the following analysis.

Genetic diversity and genetic structure

Haplotype (h ranging from 0.91 to 1) and nucleotide (π ranging from 1.69 to 6.35%) diversities for the control region were consistently high among populations (Table 2). Nucleotide diversity was the highest at Biak, and overall was higher for populations located at both extremities of the archipelago. For microsatellites, observed heterozygosities were also consistently high among populations (H_o ranging from 0.81 to 0.89), being highest at Biak. Allelic richness (A) was highest at Bali and lowest at Kupang, ranging from 8.34 to 20.

AMOVA performed with both markers showed highly structured populations, significantly deviating from panmictic conditions (mtCR: $\Phi_{st} = 0.42$, $P < 0.0001$; microsatellites: $F_{st} = 0.01$, $P < 0.0001$). Pairwise Φ_{st}- and D_{est}-values are shown in Table 3. Both markers congruent in a very strong differentiation of Biak (pairwise Φ_{st} ranging from 0.54 to 0.65; D_{est} ranging from 0.08 to 0.1) and Padang (pairwise Φ_{st} ranging from 0.62 to 0.7; D_{est} ranging from 0.09 to 0.1). Microsatellites also supported a relatively high differentiation of Karimunjawa (pairwise D_{est} ranging from 0.07 to 0.1) from the other populations.

The best supported grouping in a hierarchical AMOVA was a differentiation between Biak [Bk] and the other populations for the control region (Table 4, $\Phi_{ct} = 0.64$, $P = 0.05$), while tests performed with microsatellites rather supported the separation of Padang and Karimunjawa [Pa, Ka] additionally to Biak [Bk] from the rest of the populations ($F_{ct} = 0.05199$, $P < 0.0001$). Overall, both datasets distinguished populations from western and eastern IMA as being distinct from central ones.

Results given by STRUCTURE indicate the most probable scenario as being $k = 3$ clusters among the dataset (Fig. 1c; Supplementary Fig. S2), which could be attributable to the Western, Central and Eastern IMA. Indeed, the bar plot calculated with STRUCTURE shows a very clear differentiation of population 16 (Biak), and populations 1 and 2 (Padang and Karimunjawa, respectively) from the rest of the dataset (Fig. 1c). Pie charts depict the distribution of the genotype clusters identified across populations (Fig. 1d). Results are highly consistent with hierarchical AMOVA groupings performed with microsatellites (Table 4) and the haplotype network (Fig. 1a).

Table 2 Sample sites, abbreviations (Abbr.), and number of individuals (N_{ind}) per site for both markers in the anemonefish *Amphiprion clarkii* from the Indo-Malay Archipelago

Site	Abbr	Control region (mtCR)				Microsatellites-8 loci		
		N_{ind}	N_{hapl}	h + SD	π (%) + SD	N_{ind}	H_o + SD	A + SD
Padang	Pa	14	13	0.98 ± 0.03	1.89 ± 1.0	14	0.81 ± 0.442	14.00 ± 0.00
Karimunjawa	Ka	8	8	1.00 ± 0.06	4.61 ± 2.6	9	0.82 ± 0.453	9.057 ± 0.21
Bali	Ba	20	19	0.99 ± 0.01	4.83 ± 2.4	20	0.84 ± 0.451	20.00 ± 0.00
Taiwan	Ta	8	8	1.00 ± 0.06	1.69 ± 1.0	8	0.86 ± 0.476	8.563 ± 0.78
Banggi_Islands	BI	4	4	1.00 ± 0.17	2.39 ± 1.6	13	0.83 ± 0.453	10.97 ± 0.99
Spermonde	Sp	15	15	1.00 ± 0.02	2.46 ± 1.3	21	0.85 ± 0.457	14.52 ± 1.83
Donggala	Do	20	20	1.00 ± 0.01	2.45 ± 1.3	19	0.83 ± 0.444	19.00 ± 0.00
Togian Islands	TI	9	9	1.00 ± 0.05	2.59 ± 1.4	17	0.82 ± 0.442	12.43 ± 0.96
Kendari	Ke	8	7	0.96 ± 0.07	2.29 ± 1.3	10	0.83 ± 0.464	9.824 ± 0.48
Luwuk	Lu	14	12	0.96 ± 0.04	1.74 ± 0.9	14	0.84 ± 0.453	13.75 ± 0.25
Manado	Ma	9	8	0.97 ± 0.06	2.27 ± 1.3	17	0.86 ± 0.470	11.98 ± 1.79
Kupang	Ku	10	9	0.97 ± 0.05	1.91 ± 1.0	10	0.86 ± 0.471	8.335 ± 0.34
Misool	Mi	10	7	0.91 ± 0.07	3.64 ± 2.0	10	0.86 ± 0.472	10.43 ± 1.42
Pisang	Pi	9	7	0.94 ± 0.07	2.45 ± 1.4	10	0.85 ± 0.466	10.00 ± 0.00
Triton Bay	TB	19	18	0.99 ± 0.01	1.94 ± 1.0	6	0.81 ± 0.463	5.541 ± 0.98
Biak	Bk	21	16	0.96 ± 0.02	6.35 ± 3.2	19	0.89 ± 0.471	17.56 ± 2.41

Number of haplotypes (N_{hapl}), nucleotide (π) and haplotype (h) diversity for mtCR, observed heterosigosity (H_o) and mean allelic richness (A) for polymorphic microsatellites. SD, standard deviation

Haplotype network

The haplotype network drawn from the 209 mtCR DNA sequences (Fig. 1a) showed four haplogroups (A, B, C and D), separated by 14, 40, and 42 mutations. The most abundant one was haplogroup A, which was encountered at 14 out of 16 sample sites. It is mostly distributed throughout the central IMA, from Karimunjawa to Triton Bay. Eleven stations exclusively display this haplogroup, especially in Sulawesi where only this one was found. Due to its wide distribution and its important presence among populations, it is most likely to contain ancestral haplotypes. Haplogroup B was exclusively found at Biak. This sample site harbours haplogroups B and D, which differ by 40 and 42 mutations from haplogroup A, respectively. This makes the sample site from Biak particularly differentiated from the others. Haplogroup C was found throughout the Western IMA, from Bali to Padang. Haplogroup D is the smallest one and was only distributed in Biak and Misool. Most of the populations only harbour one haplogroup (Fig. 1b), which shows a very clear genetic structure across the IMA, and strong differentiations occurring among the Western, Central and Eastern IMA.

Bidirectional gene flow

Gene flow estimates are presented in Table 5 for each pair of populations, and all are robust as the minimal ESS value is always greater than 50. Most of the estimated gene flow values are extremely low, with more than a third being 0. Overall, this shows that there is virtually no gene flow among populations of *A. clarkii* within the IMA.

Discussion

Genetic structure

The genetic breaks identified across the IMA for Clark's anemonefish are consistent with those existing for congeneric species from the same region (*A. ocellaris*, Timm and Kochzius 2008; Timm et al. 2012; *A. perideraion*, Dohna et al. 2015; and also several other coral reef taxa, such as giant clams (*Tridacna crocea*: Kochzius and Nuryanto 2009, Hui et al. 2017; *T. maxima*: Nuryanto and Kochzius 2009; *T. squamosa*: Hui et al. 2016), corals (*Heliofungia actiniformis*: Knittweis et al. 2009; *Seriatopora hystrix*: van der Ven et al. 2021), a sea star (*Linckia laevigata*: Crandall et al. 2008, Kochzius et al. 2009) and reef fish (*Caesio cuning*: Ackiss et al. 2013; *Dascyllus aruanus*: Raynal et al. 2014). The haplotype network and hierarchical AMOVA groupings provide a clear pattern of genetic differentiation among the Western, Central and Eastern IMA (Table 4, Fig. 1a). This is confirmed by the STRUCTURE analysis (Fig. 1c), as three clusters were clearly identified. Padang and Karimunjawa form the western group, and Biak alone forms the eastern group. These three sample sites also show high pairwise Φ_{st} and

Table 3 Pairwise Φ_{st} (below diagonal) and D_{est} (above diagonal) values for the mitochondrial control region marker and microsatellites, respectively, in the anemonefish *Amphiprion clarkii* from the Indo-Malay Archipelago

mtCR\Msat	Mi	Pi	Pa	Ta	TB	Sp	Ka	TI	Bk	Ma	Ke	BI	Ba	Ku	Do	Lu	
Mi		0.046	**0.102**	0.055	0.049	**0.048**	0.094	**0.059**	0.079	**0.056**	0.040	0.054	**0.059**	0.033	**0.058**	**0.052**	Mi
Pi	**0.02459**		0.105	**0.049**	0.060	0.047	0.097	0.070	0.093	0.072	**0.038**	0.049	0.057	0.056	0.060	0.061	Pi
Pa	0.62796	**0.68618**		0.094	0.111	**0.092**	**0.038**	**0.111**	**0.103**	0.104	0.088	**0.092**	0.062	**0.100**	**0.101**	0.107	Pa
Ta	**0.12941**	0.07809	**0.699**		0.041	0.027	0.083	**0.046**	0.085	**0.046**	0.039	0.039	0.048	0.035	0.036	**0.039**	Ta
TB	0.02639	0.00011	0.69259	0.0843		0.026	0.094	0.051	0.081	**0.042**	**0.038**	**0.033**	**0.054**	0.038	**0.031**	0.040	TB
Sp	**0.13907**	**0.09419**	**0.64781**	0.00582	0.06942		**0.080**	0.038	**0.076**	**0.033**	0.028	**0.025**	0.042	**0.029**	0.028	0.031	Sp
Ka	0.20055	0.23723	0.31374	0.22803	**0.27314**	0.22178		**0.098**	**0.102**	0.085	**0.074**	**0.084**	0.057	0.084	0.083	0.091	Ka
TI	**0.07254**	0.01429	0.65645	**0.02688**	0.02665	0.5859	0.18234		0.102	0.038	0.039	0.056	**0.062**	0.042	**0.050**	**0.039**	TI
Bk	0.53986	**0.59663**	**0.64612**	**0.60124**	0.65418	0.62368	**0.54213**	0.05226		**0.097**	**0.081**	0.084	0.091	0.079	0.093	**0.094**	Bk
Ma	0.10104	0.07258	0.68536	0.09065	**0.06432**	**0.03492**	0.19938	0.0271	0.60784		0.036	0.045	0.053	**0.037**	0.036	0.037	Ma
Ke	0.13413	**0.12194**	**0.65236**	**0.06286**	0.09038	0.00124	0.17919	0.00841	**0.58604**	0.08105		0.033	**0.040**	**0.033**	**0.033**	**0.035**	Ke
BI	0.07411	0.08791	0.64207	0.05557	0.07649	**0.0227**	0.10373	**0.01119**	0.53913	0.03226	**0.02487**		0.042	0.040	0.037	0.044	BI
Ba	**0.27854**	**0.28986**	0.15918	**0.257**	0.32029	0.26342	**0.00112**	0.24769	0.56111	**0.28118**	0.22313	0.16201		0.051	**0.049**	0.053	Ba
Ku	**0.12353**	**0.08545**	0.67728	0.04055	**0.06843**	0.01812	0.2003	− 0.0074	**0.60197**	0.05226	**0.0294**	− 0.0161	**0.25144**		0.037	**0.034**	Ku
Do	0.10852	0.05355	**0.62359**	0.00441	0.03295	− 0.0038	0.18223	**0.01239**	0.63329	**0.01045**	− 0.0044	**0.03073**	0.245	**0.0103**		**0.041**	Do
Lu	**0.12641**	0.08069	**0.69612**	**0.02683**	0.05651	0.04616	**0.24243**	− 0.0071	**0.62765**	0.07611	**0.01711**	0.06728	0.28569	− 0.0341	0.00292		Lu
	Mi	Pi	Pa	Ta	TB	Sp	Ka	TI	Bk	Ma	Ke	BI	Ba	Ku	Do	Lu	

Bold values are significant ($P < 005$)

Table 4 Hierarchical AMOVA groupings for different scenarios with both mtCR and microsatellites in the anemonefish *Amphiprion clarkii* from the Indo-Malay Archipelago

# Groups	Groupings	Control region D-loop		Microsatellites-8 loci	
		Φ_{ct}	P	F_{ct}	P
2	[Bk][all others]	**0.63852**	**0.04692**	0.04341	0.06647
	[Pa][all others]	0.30207	0.11241	0.03851	0.11632
	[Bk,Mi][Pa][all others]	0.36895	0.08504	0.02485	0.02933
3	[Pa][Bk][all others]	0.62545	0.01369	0.04829	0.01271
	[Pa,Ka,Ba][Bk][all others]	0.42871	0.01095	0.03001	< 0.0001
	[Pa,Ka][Bk][all others]	0.58028	0.00098	**0.05199**	**< 0.0001**
	[Bk][Mi][Ka,Pa][all others]	0.53686	0.00782	0.04590	< 0.0001
4	[Bk][Mi][Pa][all others]	0.57371	0.01857	0.04067	0.00782
	[Bk,Mi][Pi][Pa,Ka][all others]	0.38269	0.05474	0.03889	0.00098
	[Bk,Mi][TB][Pa][all others]	0.25804	0.01003	0.01953	0.04203

Bold values indicate combinations providing the highest significant Φ_{ct} value for each marker

Table 5 Gene flow estimates for the studied pairs of *Amphiprion clarkii* populations from the Indo-Malay Archipelago

Populations (1–2)	$m_{1->2}$	$m_{2->1}$	Min (ESS)
Karimujawa-Bali	0.00003	0.00006	116
Bali-Kendari	0	0.00027	124
Kendari-Misol	0.00001	0	203
Misol-Biak	0	0.00001	285
Spermonde-Banggi Islands	0.00034	0.00027	697
Bali-Biak	0	0	397

$m_{1->2}$ is the gene flow from population 1 to 2, $m_{2->1}$ is the gene flow from population 2 to 1. This table also shows minimal ESS values for each run

D_{est}-values (Table 3). Highly restricted exchange was also confirmed by analysis of bidirectional gene flow (Table 5). Overall, these groupings are also consistent with the biogeographic coastal provinces defined by Spalding et al. (2007), supporting the idea that current differentiation patterns are influenced by historical climatic events.

Regarding the Western IMA, results support the differentiation of samples of the Eastern Indian Ocean (Padang) and Java Sea (Karimunjawa) from the central archipelago. Hierarchical AMOVA groupings performed with microsatellites and the analysis performed with STRUCTURE group these populations together (Table 4, Fig. 1c), although disagreements with mtCR marker exist. This genetic barrier has been identified for two *Amphiprion* species (*A. ocellaris*: Timm and Kochzius 2008, Timm et al. 2012; *A. perideraion*: Dohna et al. 2015). The formation of a massive land barrier along the current Indonesian islands (Fig. 1b, light grey areas) has already been identified as a cause of allopatric speciation among populations (McMillan and Palumbi 1995; Kochzius et al. 2003), through fluctuations of sea level and fragmentation of habitat during the Pleistocene (Voris 2000). This study shows that this historical genetic break still exists due to a contemporary oceanographic barrier. In a biophysical modelling approach, it was shown that sea surface currents (SSC) prevent larvae to travel from the Flores Sea to the Java Sea, causing its populations to remain isolated (Kool et al. 2011). Microsatellite markers confirm a high differentiation occurring among Western and Central populations, suggesting a continued isolation of populations of the Java Sea from the rest of the IMA. This supports the idea that old vicariant events still remain today, and act upon the genetic differentiation pattern of marine species.

Populations from the central part of the IMA only hold haplogroup A haplotypes (Fig. 1), while populations of congeneric species of the same region share several haplogroups (*Amphiprion ocellaris*: eight haplogroups, Timm and Kochzius 2008; *Amphiprion perideraion*: nine haplogroups, Dohna et al. 2015). Populations of *A. ocellaris* even display a genetic differentiation between the northern (Philippines, Sulu Sea) and southern (Sulawesi, Nusa Tenggara) IMA, which is explained by a shorter PLD than its congeners (Madduppa et al. 2014a, b). The pattern obtained for populations of Clark's anemonefish might be due to the longer PLD of that species (Ye et al. 2011), providing a greater dispersal potential leading to a more homogenised genetic variation. This longer PLD might also explain the connectivity occurring among the central IMA and populations from western New Guinea (Triton Bay, Misool). These localities belong to the eastern group for congeneric species, while hierarchical AMOVA groupings and STRUCTURE analysis of Clark's anemonefish (Table 4, Fig. 1d) show that these populations of that species belong to the central group.

As for the eastern IMA, the highest significant Φ_{ct}-values obtained from hierarchical AMOVA groupings with both markers were obtained when Biak alone forms the

eastern group. Similar groupings were identified for congeneric anemonefish species. Regarding *A. perideraion*, (Dohna et al. 2015), microsatellite data group this population alone, while mtCR data also include Pisang and Triton Bay as part of the eastern group. The particular genetic diversity of populations from Misool has already been mentioned (Dohna et al. 2015). The current study also provides evidence of a specific genetic diversity, as this population is the only one to harbour haplogroup D haplotypes, besides Biak (Fig. 1), although virtually no current gene flow occurs among Misool and Biak. Further studies should focus on the small-scale genetic structure of the populations located in this region. Moreover, the haplotype network and pairwise differentiation values indicate Biak as being the most distant population (Fig. 1: 40 and 42 mutations). The very high number of mutational steps among Biak and the rest of the dataset might indicate allopatric speciation occurring within this region, and the population from Biak forming a new cryptic species.

Limited gene flow

Limited current gene flow caused local isolation and populations to evolve almost independently, shaping a strong and clear genetic structure across the IMA (Fig. 1). Gene flow is overall lower among the three different regions of the IMA (Western, Central and Eastern part) than within regions. This overall restricted gene flow in anemonefish is commonly attributed to their short PLD (Timm and Kochzius 2008; Dohna et al. 2015; Huyghe and Kochzius 2017; Timm et al. 2017), their high rate of self-recruitment (Madduppa et al. 2014a, b) and oceanographic barriers (Kool et al. 2011; Huyghe and Kochzius 2018). As an example, the strong differentiation of Biak could be explained by the formation of the Halmahera Eddy, acting as an oceanographic barrier and leading to the isolation of this population. The biophysical dispersal model simulations from Kool et al. (2011) showed evidence of limited exchange potential between this site and other populations in the IMA and highlights the overall importance of SSC for the connectivity of marine species in this region. Moreover, the patterns obtained with simulated larvae clearly match with the direction and the intensity of SSC occurring within this region (Fig. 1b, d) (Kool et al. 2011).

Conservation perspectives

Overall, the current study shows very limited gene flow among populations, recent population separation times on an evolutionary time scale and consistently high haplotype diversity and observed heterozygosity. Together these factors, as well as the strong genetic differentiation occurring between the different regions of the IMA, provide valuable information from a conservation standpoint. The existence of barriers to gene flow, as well as the persistence of the phylogeographic barriers among Western, Central and Eastern IMA, should be considered in the design of MPA networks. Very limited exchange exists among populations located at each side of the genetic breaks, thus leading to local isolation. Additionally, the high level of self-recruitment in this taxon (Beldade et al. 2012; Madduppa et al. 2014a, b) enhances the need to act at a smaller scale, as populations may also require specific efforts on top of designing MPA networks. For instance, the population of Clark's anemonefish from Biak is highly differentiated, and virtually no gene flow occurs with adjacent populations. According to this, the limitation of anthropogenic threats such as reef exploitation, over-harvesting and gas emissions leading to temperature increase and ocean acidification is crucial for the conservation of this genetic diversity hotspot. The conservation of host sea anemones must also be considered, as the removal of this symbionts restrains larvae settlement, thus lowering population size. Resilience of marine species after habitat degradation has already been demonstrated (Barber et al. 2002), but one must lower anthropogenic effects at large scale to see populations replenish.

Supplementary Information The online version contains supplementary material available at https://doi.org/10.1007/s00338-021-02205-8.

Acknowledgements We would like to thank the Erasmus Mundus Masters Course "TROPIMUNDO" for granting a master thesis scholarship to H.D.; the German Federal Ministry of Education and Research (BMBF, Grant Nos. 03F0390B, 03F0472B and 03F0643B) for funding in the framework of the German-Indonesian project "Science for the Protection of Indonesian Coastal Ecosystems (SPICE)"; D. Blohm (Universität Bremen, Germany) for support and sub-project coordination; Leibniz Centre for Tropical Marine Research (Bremen, Germany) for support, cooperation, and project coordination; J. Jompa, scientists and students of the Hasanuddin University (Makassar, Indonesia) for logistics and help during field work; the competent Indonesian authorities for permits. The SPICE project was conducted and permitted under the governmental agreement between the BMBF and the Indonesian Ministry for Research and Technology (RISTEK), Indonesian Institute of Sciences (LIPI), Indonesian Ministry of Maritime Affairs and Fisheries (DKP) and Indonesian Agency for the Assessment and Application of Technology (BPPT). We also thank two anonymous reviewers for their comments and corrections.

Declarations

Conflict of interest On behalf of all authors, the corresponding author states that there is no conflict of interest.

References

Ackiss AS, Pardede S, Crandall ED, Ambariyanto A-L, Romena N, Barber PH, Carpenter KE (2013) Pronounced genetic structure in

a highly mobile coral reef fish, *Caesio cuning*, in the Coral Triangle. Mar Ecol Prog Ser 480:185–197

Almany GR, Berumen ML, Thorrold SR, Planes S, Jones GP (2007) Local replenishment of coral reef fish populations in a marine reserve. Science 316:742–744

Barber PH, Moosa MK, Palumbi SR (2002) Rapid recovery of genetic diversity of stomatopod populations on Krakatau: temporal and spatial scales of marine larval dispersal. Proc R Soc Lond B 269:1591–1597

Beldade R, Holbrook SJ, Schmitt RJ, Planes S, Malone D, Bernardi G (2012) Larger female fish contribute disproportionately more to self-replenishment. Proc R Soc B 279:2116–2121

Benjamini Y, Hochberg Y (1995) Controlling the false discovery rate: a practical and powerful approach to multiple testing. J R Stat Soc Ser B Stat Methodol 57:289–300

Buston PM, Bogdanowicz AW, Harrison RG (2007) Are clownfish groups composed of close relatives? An analysis of microsatellite DNA variation in *Amphiprion percula*. Mol Ecol 16:3671–3678

Clement M, Posada D, Crandall KA (2000) TCS: a computer program to estimate gene genealogies. Mol Ecol 9:1667–1669

Crandall ED, Jones ME, Munoz MM, Akinrobe B, Erdmann MV, Barber PH (2008) Comparative phylogeography of two seastars and their ectosymbionts within the Coral Triangle. Mol Ecol 17:5276–5290

Dawson MN (2014) Natural experiments and meta-analyses in comparative phylogeography. J Biogeogr 41:52–65

Dawson MN, Hays CG, Grosberg RK, Raimondi PT (2014) Dispersal potential and population genetic structure in the marine intertidal of the eastern North Pacific. Ecol Monogr 84:435–456

Dohna TA, Timm J, Hamid L, Kochzius M (2015) Limited connectivity and a phylogeographic break characterize populations of the pink anemonefish, *Amphiprion perideraion*, in the Indo-Malay Archipelago: inferences from a mitochondrial and microsatellite loci. Ecol Evol 5:1717–1733

Fu YX (1997) Statistical tests of neutrality of mutations against population growth, hitchhiking and background selection. Genetics 147:915–925

Hey J, Nielsen R (2007) Integration within the Felsenstein equation for improved Markov chain Monte Carlo methods in population genetics. Proc Natl Acad Sci USA 104(8):2785–2790

Hui M, Kraemer WE, Seidel C, Nuryanto A, Joshi A, Kochzius M (2016) Comparative genetic population structure of three endangered giant clams (Tridacnidae) throughout the Indo-West Pacific: implications for divergence, connectivity, and conservation. J Molluscan Stud 82:403–414

Hui M, Nuryanto A, Kochzius M (2017) Concordance of microsatellite and mitochondrial DNA markers in detecting genetic population structure in the boring giant clam, *Tridacna crocea*, across the Indo-Malay Archipelago. Mar Ecol 38:e12389

Huyghe F, Kochzius M (2017) Highly restricted gene flow between disjunct populations of the skunk clownfish (*Amphiprion akallopisos*) in the Indian Ocean. Mar Ecol 38:e12357

Huyghe F, Kochzius M (2018) Sea surface currents and geographic isolation shape the genetic population structure of a coral reef fish in the Indian Ocean. PLoS ONE 13:e0193825

Jones GP, Planes S, Thorrold SR (2005) Coral reef fish larvae settle close to home. Curr Biol 15:131421318

Knittweis L, Kraemer WE, Timm J, Kochzius M (2009) Genetic structure of *Heliofungia actiniformis* (Scleractinia: Fungiidae) populations in the Indo-Malay Archipelago: implications for live coral trade management efforts. Conserv Genet 10:241–249

Kochzius M, Söller R, Khalaf MA, Blohm D (2003) Molecular phylogeny of the lionfish genera *Dendrochirus* and *Pterois* (Scorpaenidae, Pteroinae) based on mitochondrial DNA sequences. Mol Phylogenet Evol 28:396–403

Kochzius M, Nuryanto A (2009) Strong genetic population structure in the boring giant clam, *Tridacna crocea*, across the Indo-Malay Archipelago: implications related to evolutionary processes and connectivity. Mol Ecol 17:3775–3787

Kochzius M, Seidel C, Hauschild J, Kirchhoff S, Mester P, Meyer-Wachsmuth I, Nuryanto A, Timm J (2009) Genetic population structures of the blue starfish *Linckia laevigata* and its gastropod ectoparasite *Thyca crystallina*. Mar Ecol Prog Ser 396:211–219

Kool JT, Paris CB, Barber PH, Cowen RK (2011) Connectivity and the development of population genetic structure in Indo-West Pacific coral reef communities: Indo-West Pacific connectivity. Glob Ecol Biogeogr 20:695–706

Lee W-J, Conroy J, Howell WH, ThomasD K (1995) Structure and evolution of teleost mitochondrial control regions. J Mol Evol 41:54–66

Liu SYV, Yu HT, Dai CF (2007) Eight microsatellite loci in Clark's anemonefish, *Amphiprion clarkii*. Mol Ecol Notes 7:1169–1171

Madduppa HH, Timm J, Kochzius M (2014a) Interspecific, spatial and temporal variability of self-recruitment in anemonefishes. PLoS ONE 9:12

Madduppa HH, von Juterzenka K, Syakir M, Kochzius M (2014b) Socio-economy of marine ornamental fishery and its impact on the population structure of the clown anemonefish *Amphiprion ocellaris* and its host anemones in Spermonde Archipelago, Indonesia. Ocean Coast Manag 100:41–50

Madduppa HH, Timm J, Kochzius M (2018) Reduced genetic diversity in the clown anemonefish *Amphiprion ocellaris* in exploited reefs of Spermonde Archipelago, Indonesia. Front Mar Sci 5:80

McMillan WO, Palumbi SR (1995) Concordant evolutionary patterns among Indo-West Pacific butterflyfishes. Proc R Soc Lond B 260:229–236

Nei M (1987) Molecular evolutionary genetics. Columbia University Press, New York

Nuryanto A, Kochzius M (2009) Highly restricted gene flow and deep evolutionary lineages in the giant clam *Tridacna maxima*. Coral Reefs 28:607–619

Pinsky ML, Montes HR Jr, Palumbi SR (2010) Using isolation by distance and effective density to estimate dispersal scales in anemonefish. Evolution 64(9):2688–2700

Planes S, Jones GP, Thorrold SR (2009) Larval dispersal connects fish populations in a network of marine protected areas. Proc Natl Acad Sci USA 106:5693–5697

Quenouille B, Bouchenak-Khelladi Y, Hervet C, Planes S (2004) Eleven microsatellite loci for the saddleback clownfish *Amphiprion polymnus*. Mol Ecol Notes 4:291–293

Ray N, Currat M, Excoffier L (2003) Intra-deme molecular diversity in spatially expanding populations. Mol Biol Evol 20:76–86

Raynal R, Crandall ED, Barber PH, Mahardika G, Lagman M, Carpenter KE (2014) Basin isolation and oceanographic features influencing lineage diversification in the humbug damselfish (*Dascyllus aruanus*) in the Coral Triangle. Bull Mar Sci 90:513–532

Spalding MD, Fox HE, Allen GR, Davidson N, Ferdaña ZA, Finlayson M, Halpern BS, Jorge MA, Lombana A, Lourie SA, Martin KD, Molnar J, Recchia CA, Robertson J (2007) Marine Eecoregions of the world: a bioregionalization of coastal and shelf areas. Biosci J 57:573–583

Simpson SD, Harrison HB, Claereboudt MR, Planes S (2014) Long-distance dispersal via ocean currents connects clownfish populations throughout entire species range. PLoS ONE 9:e107610

Slatkin M, Excoffier L (1996) Testing for linkage disequilibrium in genotypic data using the expectation-maximization algorithm. Heredity 4:77–383

Tajima F (1989) Statistical method for testing the neutral mutation hypothesis by DNA polymorphism. Genetics 3:585–595

Timm J, Kochzius M (2008) Geological history and oceanography of the Indo-Malay Archipelago shape the genetic population structure in the false clown anemonefish (*Amphiprion ocellaris*). Mol Ecol 17:3999–4014

Timm J, Planes S, Kochzius M (2012) High similarity of genetic population structure in the false clown anemonefish (*Amphiprion ocellaris*) found in microsatellite and mitochondrial control region analysis. Conserv Genet 13:693–706

Timm J, Kochzius M, Madduppa HH, Neuhaus AI, Dohna T (2017) Small-scale genetic population structure of coral reef organisms in Spermonde Archipelago. Indonesia Front Mar Sci 4:294

van der Ven RM, Heynderickx H, Kochzius M (2021) Differences in genetic diversity and divergence between brooding and broadcast spawning corals across two spatial scales in the Coral Triangle region. Mar Biol 168:17

Voris HK (2000) Maps of Pleistocene sea levels in Southeast Asia: shorelines, river systems and time durations. J Biogeography 27:1153–1167

Wright S (1965) The interpretation of population structure by F-statistics with special regard to systems of mating. Evolution 19:395–420

Ye L, Yang SY, Zhu XM, Liu M, Lin JY, Wu KC (2011) Effects of temperature on survival, development, growth and feeding of larvae of Yellowtail clownfish *Amphiprion clarkii* (Pisces: Perciformes). Acta Ecol Sin 31:241–245